PHYSICAL REVIEW B **90**, 220102(R) (2014)

Decoupling of defect and short-range order contributions to resistivity recovery measurements in binary alloys

B. Gómez-Ferrer,[1,2,3,*] I. García-Cortés,[1] J. F. Marco,[4] D. Jiménez-Rey,[1,3] and R. Vila[1]
[1]*Laboratorio Nacional de Fusión, CIEMAT, Avenida Complutense 40, 28040 Madrid, Spain*
[2]*UNED, Fundación & Departamento Ingeniería Energética, Madrid, Spain*
[3]*Centro de Micro-Análisis de Materiales, Universidad Autónoma de Madrid, 28049 Madrid, Spain*
[4]*Instituto de Química Física "Rocasolano," CSIC, Calle Serrano 119, 28006 Madrid, Spain*
(Received 1 July 2014; published 2 December 2014)

We report a new and improved approach that uses low-temperature resistivity recovery measurements to study the defect kinetics in metallic binary alloys. This method is able to decouple the effect related to the irradiation defect contribution to the resistivity from that of the short-range order, which is enhanced by the free migration of defects. This approach can provide reliable experimental data which are more suitable for comparisons with current computational models. Furthermore, the difference in this method with respect to the classical one is that our method gives information concerning the role of vacancies and interstitials on short-range order. The method is applied to a model alloy Fe-5%Cr, of interest for fusion applications, where short-range order effects have been previously found to play a role.

DOI: 10.1103/PhysRevB.90.220102 PACS number(s): 75.40.−s, 72.15.Eb, 72.80.Ga, 76.80.+y

In general, concentrated alloys have enough solute concentration to perturb the electronic structure and the phonon spectrum. Typically this composition range starts at 1%–2% of the solute concentration. These perturbations lead to an atomic configuration which is never fully random; there are certain atomic correlations that can be described as short-range order (SRO). The SRO parameters (α_i) are defined as the correlation between first- and next-nearest neighbors (NN) of an atom [1]. Every alloy has different SRO equilibrium configurations for every solute concentration and temperature [2], which also depend on the thermomechanical process experienced [3,4]. Quenching experiments have been widely used to study the kinetics of ordering [2–8] given the linear relation of the resistivity (ρ) with α_i (cf. Refs. [1,8]). Concurrently, resistivity recovery (RR) experiments have been commonly used to investigate radiation effects in pure metals, based on the recovery of the residual resistivity up to its original value after low-temperature irradiation and subsequent isochronal annealing [9–17]. However, in the case of concentrated alloys, the presence of migrating defects allows solute rearrangements and changes in the SRO, which in turn affect the residual resistivity of the alloy. This effect might thus significantly alter the RR results and their interpretation, as it has been discussed in the case of Fe-Cr [18,19].

In the field of energy advanced materials development there is specific interest in the study of Cr effects on nuclear alloys [20,21], given that Cr concentrations (C_{Cr}) close to 9% reduce swelling [22,23], reduce the radiation-induced ductile-brittle transition temperature (DBTT) [24], and increase protection against corrosion [25]. The physics of these effects is not yet well understood though it is believed that the minimum of the SRO parameters might play a role in affecting the kinetics of radiation defects in a concentrated Fe-Cr system. Indeed, it has been proven that α_i change their sign at C_{Cr} close to 10% [26–28]. At $C_{Cr} < 11\%$ the SRO becomes negative, i.e., Cr tends to distribute as far as possible in the Fe matrix (ordering), probably because of a magnetic frustration effect [27,29]. At increasing Cr concentrations ($C_{Cr} > 11\%$), the number of configurations which maximize the Cr-Cr separation start to decrease. Then Cr atoms tend to clusterize, changing the sign of the SRO parameters. The dependence of SRO on C_{Cr} and temperature leads to a miscibility gap of the Fe-Cr phase diagram where the bcc structure starts to decompose in two phases, α and α', enriched with Fe and Cr, respectively [28,30] with important implications on the metallurgical structure.

The RR experiments are being used as a complementary tool to address the design of structural steels and divertor armor materials. Concurrently to materials engineering, many efforts are dedicated to the understanding of the physical processes responsible for the radiation degradation processes [31–34], based on multiscale modeling, together with validation experiments. In this regard, RR experiments are used as validation experiments to monitor the changes in defect populations, which can also be reproduced by modeling simulations [13,35–39]. The well-known work of Fu *et al.* [38] demonstrated that overall agreement can be achieved between modeling [*ab initio* and kinetic Monte Carlo (KMC)] and experiments (RR and positron annihilation [13,40]) in the case of electron-irradiated ultrapure Fe. However, current physical models are not yet able to reproduce RR data when it comes to concentrated alloys and irradiations with high-energy primary knock-on atoms.

In order to fully understand the defect kinetics in Fe-Cr systems, it is necessary to match the theoretical predictions and experiments. A recent work [39] which combines molecular dynamics (MD), atomistic KMC (AKMC) coupled to a neural network, and rate theory (RT) succeeded in reproducing several experimental results of RR in dilute [35,36] and concentrated electron-irradiated Fe-Cr alloys [37]. That work reproduces well the recovery stages due to correlated recombinations but has a limited range of application given that it only simulates a single recombination process in stage II and is not able to accurately reproduce the amplitude of stage III. This last limitation is, as the authors state, probably due to SRO

*begona.gomez-ferrer@externos.ciemat.es

effects which are not included in the model. This is actually one of the main limitations of computational simulations that are devoted to reproducing RR results, because they assume that resistivity is only driven by the defect populations (along the postirradiation thermal annealing). Accurate models such as AKMC and MD still cannot calculate the proper value of the residual resistivity of an alloy depending on its nonrandom solute distribution (ρ_{SRO}). On the other hand, object KMC (OKMC) and RT which do not take into account the local environment are even further away from being able to reproduce such SRO effects.

Given the distortions that SRO makes in RR peaks and the limitations of the current computational methods to calculate the ρ_{SRO} contribution, we have conceived an important modification upon the traditional RR method which might be able to eliminate the effects of SRO contributions to the RR curves. In this Rapid Communication we present the first measurement of a RR curve where this SRO contribution has been highly reduced. The method is described below.

As stated, the electrical resistivity depends sensitively on the concentration of defects and solute arrangements. A typical RR experiment consists of low-temperature irradiation (below 70 K) of well-prepared specimens of small dimensions. By measuring the resistivity at cryogenic temperatures, the phonon and magnetic contributions are strongly reduced and the defect contribution is revealed [8]:

$$\rho = \rho_0 + \rho_D + \rho_{SRO}, \quad (1)$$

where ρ_0 is the residual resistivity of the metal free of irradiation defects, ρ_D is the resistivity contribution of point defects, and ρ_{SRO} is a contribution associated with the SRO state. The followup of this value after irradiation, along with isochronal thermal annealing, shows the reduction of resistivity at different temperature stages related to different thermally activated mechanisms, such as migration, recombination, clustering, and dissociation of various defect types. This picture works very well in pure and dilute metal alloys where ρ_{SRO} can be neglected. However, in concentrated alloys the stages related to the free migration of interstitials and vacancies favor a local redistribution of solutes, leading to large variations in ρ_{SRO} [19,41,42]. The method proposed in the present work consists of performing a preirradiation (pre-Irr) of the sample near the high-temperature value of the RR measurement. In the case of Fe-Cr alloys a temperature of 400 K was chosen. By irradiating at such a temperature it is known that the defects that are created have enough thermal energy to migrate and recombine (with the exception of a few clusters that might be formed). In doing so, the pre-Irr step allows the vacancies and interstitials to freely migrate in the material, enhancing the rearrangement of Cr atoms. Thus, the pre-Irr step allows the SRO configuration to reach an equilibrium state. This means that further movement of the migrating defects no longer changes the state of SRO and the ρ_{SRO} value saturates. This defines the minimum irradiation dose that must be used for this pre-Irr treatment for each alloy. The SRO saturation has been experimentally observed in many alloys, e.g., in Ni-11.4%Cr [43], which has similar features to Fe-Cr alloys. After this pre-Irr step, the sample is cooled down to liquid He temperature. Then, regular low-temperature irradiation at 50 K and subsequent isochronal annealing with a followup of resistivity is performed (RR). The advantage of using the pre-Irr step is that the sample is now close to its SRO equilibrium value. Therefore, it is expected that at temperatures where defects would migrate and SRO would normally change (in a classical RR experiment), no appreciable variation of the SRO will occur and hence no change due to ρ_{SRO} will be observed. Thus, at the end of the RR experiment, the recovery of the resistivity should be almost complete. Whether this would be observed would demonstrate that the material has come back to its original microstructural state after the pre-Irr step and thus the RR curve only shows effects due to defect migration.

The material used in this study was a high purity Fe-Cr alloy with 5.4 wt % of Cr concentration and impurity contents of C, O, S, N, and P lower than 6 ppm. The dislocation density was measured to be about $1.2 \times 10^8/\text{cm}^2$ and the mean grain size was 68 μm [44]. Samples of $\sim$50 μm thickness were cut by spark erosion and thinned by grinding and polishing in a plane-parallel polishing machine. The resistivity was measured at 20 K by the van der Pauw method [45]. To control the temperature, two type E thermocouples were spot welded to the sample and a silicon diode was placed just next to it. The sample holder was mounted in the cold finger of a continuum-flow cryostat at the end of one of the lines of the CMAM ion accelerator facility [46] where the experiments were carried out. Further details on the measurement method, sample preparation, and the microstructure can be found in Refs. [42,44]. Also, the details related to the damage created by 5 MeV protons, mainly Frenkel pairs and a few clusters, can be found in Ref. [42].

Two RR measurements were performed to prove this SRO suppression method and the results are presented in Fig. 1. The blue line (circles, "classic RR") represents the normalized RR curve of a Fe-5% Cr sample at which the classical RR method was applied, i.e., just irradiating at low temperature with 5 MeV protons (the flux is $\sim 3.5 \times 10^{11}$

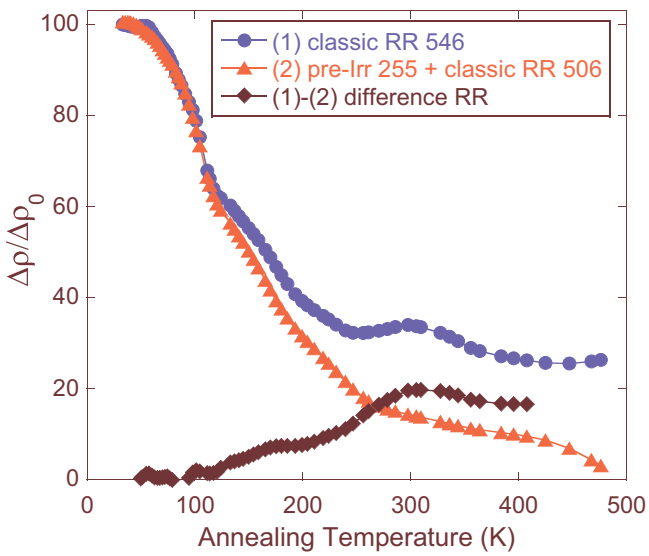

FIG. 1. (Color online) Fe-5%Cr samples irradiated with 5 MeV protons. Comparison of experimental RR curves with (●) and without (▲) SRO effects after preirradiation at 400 K.

TABLE I. Specimen experimental characteristics: thickness, initial residual resistivity (10.1 $\mu\Omega$ cm), and RIR measured at a minimum temperature reached on the sample, 23 K.

		Pre-Irr. (400 K) 240×10^{-6} dpa		Low-T Irr. (50 K) 100×10^{-6} dpa	
Thickness (μm)	% recovery at 400 K	Fluence (cm^{-2})	$\Delta\rho$ (nΩ cm)	Fluence (cm^{-2})	$\Delta\rho$ (nΩ cm)
52.0 ± 1.2	26.5			3.7×10^{15}	546
54.7 ± 1.5	10.0	10.7×10^{15}	255	3.6×10^{15}	506

cm^{-2} s^{-1}) and subsequent isochronal annealing. The effects of ordering can be appreciated because, in some temperature ranges, ρ is increasing instead of decreasing, as one would expect due to the recombination of defects, and the recovery of the resistivity is prevented up to 26.5%. The red RR curve (triangles, "pre-Irr+classic RR") corresponds to a sample prepared with the pre-Irr step described above with a flux of $\sim 1.5 \times 10^{12}$ cm^{-2} s^{-1}. Subsequently, the classical RR method was applied to this sample, just as the previous one. Therefore, as the sample is cooled down to ~20 K right after pre-Irr, the SRO state reached is frozen. A first proof of the validity of the method is that the residual resistivity value after pre-Irr (but before low-temperature irradiation) is increased by 255 nΩ cm because of the rearrangement of Cr atoms (as defects recombine and do not contribute to ρ). Furthermore, the figure clearly evidences that at the end of the thermal treatment, residual resistivity is almost recovered, in contrast to the sample where the pre-Irr step was not applied. The black line (diamonds, "difference RR") shows the difference between both RR curves and therefore evidences the SRO effects on the conventional RR curve of a concentrated alloy. Details on the characteristics of the samples, the radiation-induced resistivities, and fluences can be found in Table I. Regarding the difference RR curve, two clear stages can be observed. The first one starts at a temperature of about 100 K until it reaches a plateau, then a second increase stage in SRO is observed from 200 K and above. Although it is not the purpose of this Rapid Communication to interpret the mechanisms of the stages, the free migration of interstitials after detrapping invoked by other authors [18,39] could be responsible for the first stage, whereas the second stage, starting from 200 K, can be explained by the long-range migration of vacancies.

The impact of the RR method proposed here is also observed on RR spectra peaks (Fig. 2). First, a recovery increase is observed at stages II and III (cf. Refs. [13,38] for stage range definition) in the curve corresponding to the pre-Irr+classic RR sample with respect to the classic RR one. On the contrary, in the temperature interval between 300 and 400 K, a stage disappears in the pre-Irr+classic RR sample. These significant differences clearly evidence the importance of decoupling the real defect recombination from SRO changes. As these spectra are used to evaluate the population defect evolution—which is used to validate models—the proposed method gives very valuable information, minimizing the SRO contribution of the RR curve and therefore allowing an improved evaluation of defect recombination.

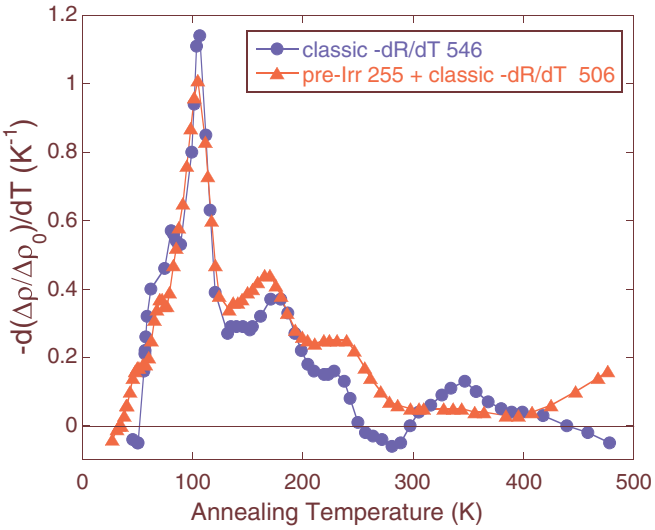

FIG. 2. (Color online) Differential RR curves of classic RR (●) and pre-Irr+classic (▲) RR samples.

In the sample pre-Irr+classic RR, during the annealing steps, some defects could again change the SRO value if the SRO equilibrium would be different at temperatures below 400 K, but, in any case, this value is the same in both samples. Therefore, the observed differences are only due to the different initial states (as received or pre-Irr). Qualitatively, such differences should be low. Otherwise, it would generate a strongly fluctuating $\rho(T)$ curve (always the sum of defect recombination and SRO changes). Moreover, the small concentration of defects created at 50 K, on a system already close to equilibrium, would generate only small changes. This hypothesis is confirmed by the experimental results as the pre-Irr sample has almost fully recovered its resistivity after isochronal annealing to the 400 K pre-Irr value. The pre-Irr+classic RR sample shows a residual resistivity value that is two times lower than the classic RR one. The small amount of residual resistivity still observed could be due to some clusters that are not yet annealed or to deviations induced by the residual concentration of defects (two current model deviations [35,47]). Above 400 K we no longer have information on the SRO. The residual resistivity of both samples should move to a new state of SRO (temperature dependent), but also the presence of the created small clusters might play a role in influencing the new SRO equilibrium states or in the appearance of new recombination stages. The total recovery of RR in the pre-Irr+classic RR sample could indicate that the original microstructural state has been fully recovered after isochronal annealing.

In order to support the arguments relative to Cr distribution, we performed a Mössbauer analysis on 30 μm thick samples of the same material and prepared following the same irradiation conditions as described before and annealed at 400 K. The spectra were recorded at room temperature using a conventional constant acceleration spectrometer and a ^{57}Co(Rh) source. The velocity scale was calibrated using a 6 μm α-Fe foil, and the isomer shifts were referred to the centroid of the spectrum of α-Fe at room temperature. The spectra of the three samples (Fig. 3) were fitted considering three magneticsextets having the following Mössbauer parameters:

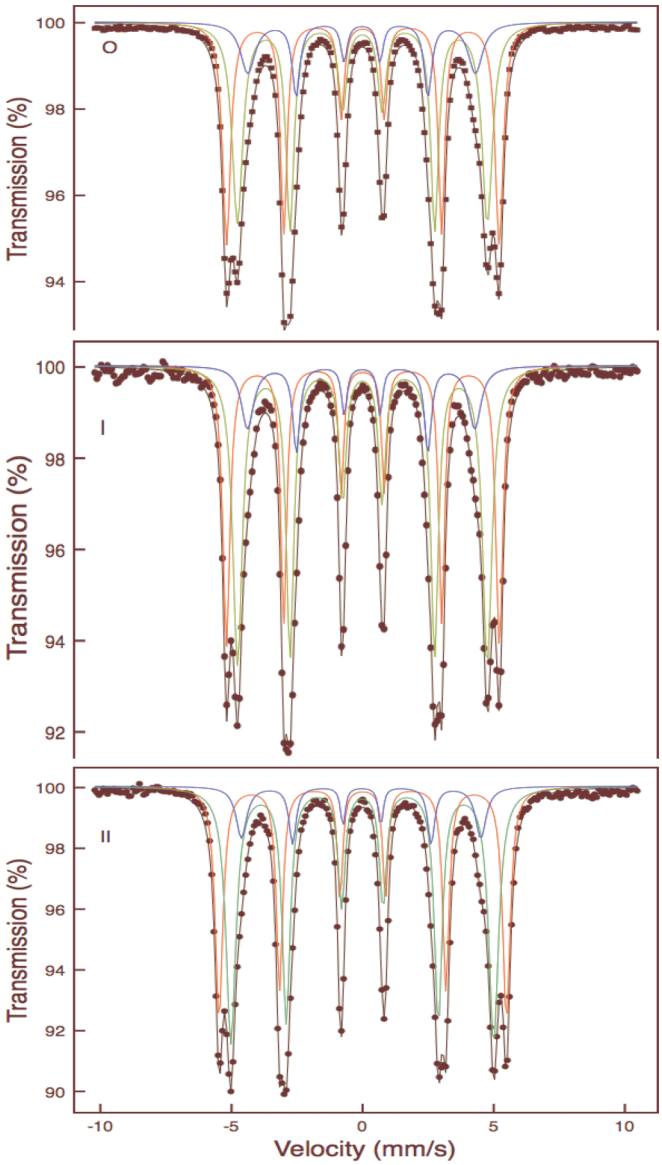

FIG. 3. (Color online) Mössbauer spectra of a Fe-5% Cr 35 μm sample measured at room temperature. The red sextet refers to the pure Fe phase, green corresponds to Fe with one Cr in the 1NN, and blue corresponds to Fe having one Cr in 1NN and one Cr in 2NN. (O) is the spectrum of the "as-received" sample, (I) is the sample after 400 K pre-Irr up to a dose of 240×10^{-6} dpa, and (II) corresponds to the sample after pre-Irr (240×10^{-6} dpa), low-T Irr (100×10^{-6} dpa), and annealing at 400 K.

$\delta_1 = 0.005$ mm s^{-1}, $2\varepsilon_1 = 0.00$ mm s^{-1}, $H_1 = 33.1$ T, $\delta_2 = -0.010$ mm s^{-1}, $2\varepsilon_2 = 0.00$ mm s^{-1}, $H_2 = 31.0$ T, $\delta_3 = -0.40$ mm s^{-1}, $2\varepsilon_3 = -0.02$ mm s^{-1}, $H_3 = 28.2$ T. The data fit well with previous interpretations [48] in which the sextet with the largest hyperfine magnetic field H_1 corresponds to Fe atoms having no Cr atoms as NN, the sextet with H_2, corresponds to Fe atoms having one Cr atom in the 1NN shell and no Cr atoms in the 2NN shell, and the sextet with H_3 represents the situation of Fe atoms with one Cr atom in the 1NN shell and one Cr atom in the 2NN shell. Inspection of Fig. 3 shows an increase in the relative area of sextet H_2: 45.6%, 50.8%, and 52.1% for the as-received, pre-Irr, and pre-Irr+RR samples, respectively. Such an increase indicates that the irradiation conditions promote the migration of Cr from the 2NN to the 1NN (the relative areas of the corresponding sextets decrease accordingly). It is clear from the data that the major change in the spectra is brought about by the preirradiation treatment and that the subsequent low-temperature irradiation treatment has only a significantly smaller influence in the final configuration of the neighboring Cr atoms. This is in good agreement with the rest of the observations of this Rapid Communication, supporting that pre-Irr almost saturates the local rearrangement of Cr atoms, allowing the sample to reach the SRO equilibrium value at 400 K.

In summary, we have proposed a novel RR measurement method to suppress the SRO contribution in the resistivity. The comparison of classical and our RR results provides experimental evidence that interstitial migration could play a role in the solute rearrangement. This fact could not be observed experimentally by quenching experiments, where SRO changes are mainly driven by thermal vacancies. The proposed method for performing RR measurements on binary alloys has been tested in the case of a Fe-5%Cr alloy, which is of interest for fusion and fission applications.

The authors acknowledge J. M. García, A. Maira, J. Narros, A. Rodríguez, and A. Muñoz for their strong technical support on irradiation and C. J. Ortiz for stimulating discussions. This work was cosupported by the European Commission (EFDA-MATREMEV work program) and Euratom/CIEMAT Association, by national program RADIAFUS (ENE2012-39787-C06-01), and Madrid Community through the project TECHNOFUSION (S2009/ENE-1679). Financial support from the Spanish Ministry of Economy and Competitiveness (project MAT2012-38045-C04-01) is also acknowledged.

[1] P. L. Rossiter, *The Electrical Resistivity of Metals and Alloys* (Cambridge University Press, Cambridge, UK, 1987).
[2] W. Kohl, R. Scheffel, H. Heidsiek, and K. Lüke, Acta Metall. **31**, 1895 (1983).
[3] W. Pfeiler, Acta Metall. **36**, 2417 (1988).
[4] E. Balanzat and J. Hillairet, J. Phys. F: Met. Phys. **11**, 1977 (1981).
[5] H. A. Schulze and K. Lücke, J. Appl. Phys. **39**, 4860 (1968).
[6] V. Pierron-Bohnes, I. Mirebeau, E. Balanzat, and M. C. Cadeville, J. Phys. F: Met. Phys. **14**, 197 (1984).
[7] R. Poerschke and W. Pfeiler, Scr. Metall. **19**, 1085 (1985).
[8] A. Schulze and K. Lücke, Acta Metall. **20**, 529 (1972).

[9] T. H. Blewitt, R. R. Coltman, and C. E. Klabunde, Aust. J. Phys. **13**, 347 (1960).
[10] J. A. Tesk, E. C. Jones, and J. W. Kauffman, Phys. Rev. **133**, A288 (1964).
[11] F. Maury, M. Biget, P. Vajda, A. Lucasson, and P. Lucasson, Radiat. Eff. **38**, 53 (1978).
[12] A. M. Omar, Ph.D. thesis, McMaster University, 1978.
[13] S. Takaki, J. Fuss, H. Kuglers, U. Dedek, and H. Schultz, Radiat. Eff. **79**, 87 (1983).
[14] H. Matsui, S. Takehana, and M. W. Guinan, J. Nucl. Mater. **155–157**, 1284 (1988).
[15] Y. Chimi, A. Iwase, and N. Ishikawa, J. Nucl. Mater. **271–272**, 236 (1999).
[16] Y. Chimi, A. Iwase, N. Ishikawa, N. Kuroda, and T. Kambara, Nucl. Instrum. Methods Phys. Res., Sect. B **164–165**, 408 (2000).
[17] H. Abe and E. Kuramoto, J. Nucl. Mater. **283–287**, 174 (2000).
[18] A. Benkaddour, O. Dimitrov, and C. Dimitrov, Mater. Sci. Forum **15–18**, 1263 (1987).
[19] A. L. Nikolaev, V. L. Arbuzov, and A. E. Davletshin, J. Phys.: Condens. Matter **9**, 4385 (1997).
[20] K. Fukuya, J. Nucl. Sci. Technol. **50**, 213 (2013).
[21] S. J. Zinkle, Fusion Eng. Des. **74**, 31 (2005).
[22] Y. Konobeev, A. Dvoriashin, S. Porollo, and F. Garner, J. Nucl. Mater. **355**, 124 (2006).
[23] S. Porollo, A. Dvoriashin, A. Vorobyev, and Y. Konobeev, J. Nucl. Mater. **256**, 247 (1998).
[24] H. Kayano, A. Kimura, M. Narui, Y. Sasaki, Y. Suzuki, and S. Ohta, J. Nucl. Mater. **155–157**, 978 (1988).
[25] M. Dusek and C. Hunt, NPL Report No. PDB: 3077, 2002 (unpublished).
[26] I. Mirebeau, M. Hennion, and G. Parette, Phys. Rev. Lett. **53**, 687 (1984).
[27] I. Mirebeau and G. Parette, Phys. Rev. B **82**, 104203 (2010).
[28] P. Erhart, A. Caro, M. Serrano de Caro, and B. Sadigh, Phys. Rev. B **77**, 134206 (2008).
[29] M. Y. Lavrentiev, R. Soulairol, C.-C. Fu, D. Nguyen-Manh, and S. L. Dudarev, Phys. Rev. B **84**, 144203 (2011).
[30] A. Caro, M. Caro, E. M. Lopasso, and D. A. Crowson, Appl. Phys. Lett. **89**, 121902 (2006).
[31] J. Boutard, M. Caturla, S. Dudarev, and F. Willaime, EFDA Report No. EFDA-D-2D4B78, 2009 (unpublished).
[32] D. Stork *et al.*, European CommissionTechnical Report No. CCEFu57-7.1, 2012 (unpublished).
[33] Ch. Linsmeier, C.-C. Fu, A. Kaprolat, S. F. Nielsen, K. Mergia, R. Schäublin, R. Lindau, H. Bolt, J.-Y. Buffière, M. J. Caturla, B. Décamps, C. Ferrero, H. Greuner, C. Hébert, T. Höschen, M. Hofmann, C. Hugenschmidt, T. Jourdan, M. Köppen, T. Płociński, J. Riesch, M. Scheel, B. Schillinger, A. Vollmer, T. Weitkamp, W. Yao, J.-H. You, and A. Zivelonghi, J. Nucl. Mater. **442**, S834 (2013).
[34] F. Romanelli *et al.*, EFDA Tech. Rep., 2013, https://www.euro-fusion.org/wpcms/wp-content/uploads/2013/02/JG12.356-web.pdf (unpublished).
[35] F. Maury, P. Lucasson, A. Lucasson, F. Faudot, and J. Bigot, J. Phys. F: Met. Phys. **17**, 1143 (1987).
[36] H. Abe and E. Kuramoto, J. Nucl. Mater. **271–272**, 209 (1999).
[37] C. Dimitrov, A. Benkaddour, C. Corbel, and P. Moser, Ann. Chim.-Sci. Mat. **16**, 319 (1991).
[38] C.-C. Fu, J. Dalla Torre, F. Willaime, J. Bocquet, and A. Barbu, Nat. Mater. **4**, 68 (2005).
[39] D. Terentyev, N. Castin, and C. J. Ortiz, J. Phys.: Condens. Matter **24**, 475404 (2012).
[40] A. Vehanen, P. Hautojärvi, J. Johansson, J. Yli-Kauppila, and P. Moser, Phys. Rev. B **25**, 762 (1982).
[41] C. Dimitrov and O. Dimitrov, J. Phys. F: Met. Phys. **14**, 793 (1984).
[42] B. Gómez-Ferrer, R. Vila, D. Jiménez-Rey, C. Ortiz, F. Mota, J. García, and A. Rodríguez, J. Nucl. Mater. **447**, 225 (2014).
[43] H. Heidsiek, R. Scheffel, and K. Lücke, J. Phys., Colloq. **38**, 174 (1977).
[44] J. Le Coze, EFDA Technical Report No. 06-1901 TW6-TTMS 007-PUREFE, ARMINES Ecole Nationale Superieure des Mines, 2007 (unpublished).
[45] L. J. van der Pauw, Philips Res. Rep. **13**, 1 (1958).
[46] A. Climent-Font, F. Pászti, G. García, M. Fernández-Jiménez, and F. Agulló, Nucl. Instrum. Methods Phys. Res., Sect. B **219–220**, 400 (2004).
[47] A. Fert and I. A. Campbell, J. Phys. F: Met. Phys. **6**, 849 (1976).
[48] S. Dubiel, J. Cieślak, and H. Reuther, Nucl. Instrum. Methods Phys. Res., Sect. B **302**, 48 (2013).